Cancer Biol Med 2025. doi: 10.20892/j.issn.2095-3941.2025.0058

ORIGINAL ARTICLE

CLT-003 exerts anti-tumor activity in pancreatic cancer by blocking the PI3K/AKT/HIF-1α pathway

Chao Xu[1,2*], Zekun Li[1*], Yueying Shan[1*], Chunhua She[1], Yanfang Yang[1], Tianxing Zhou[1], Yongjie Xie[1], Bo Ni[1], Chenyang Meng[1], Guangcong Shen[1], Boyang Fu[1], Guannan Sheng[1], Liangliang Wu[1], Jinlong Pei[1], Tiansuo Zhao[1], Song Gao[1], Hongwei Wang[1], Chengqi Deng[3], Kaiyuan Wang[3], Antao Chang[1], Chongbiao Huang[1], Lei Shi[4], Shengyu Yang[5], Jun Yu[1], Jihui Hao[1], Xiuchao Wang[1]

[1]Pancreas Center, Tianjin Medical University Cancer Institute and Hospital, National Clinical Research Center for Cancer, State Key Laboratory of Druggability Evaluation and Systematic Translational Medicine, Tianjin Key Laboratory of Digestive Cancer, Tianjin's Clinical Research Center for Cancer, Tianjin 300060, China; [2]National Clinical Research Center for Cancer, Tianjin Cancer Hospital Airport Hospital, Tianjin 300060, China; [3]Department of Anesthesiology, Tianjin Medical University Cancer Institute and Hospital, National Clinical Research Center for Cancer, Key Laboratory of Cancer Prevention and Therapy, Tianjin's Clinical Research Center for Cancer, Tianjin 300060, China; [4]Department of Biochemistry and Molecular Biology, School of Basic Medical Sciences, Tianjin Medical University, Tianjin 300070, China; [5]Department of Cellular and Molecular Physiology, Penn State College of Medicine, Hershey, Pennsylvania 17033, USA

ABSTRACT

Objective: CLT-003 is a novel phenylphthalimide derivative encapsulated in poly (lactate-glycolic acid) copolymer nanoparticles using nanotechnology techniques. CLT-003 possesses anti-angiogenetic and antitumor activities. Nevertheless, the role and molecular mechanism underlying CLT-003 in pancreatic cancer remain to be elucidated.

Methods: Cell proliferation and apoptosis were detected using CCK-8, real-time cell analysis (RTCA), EdU, and flow cytometric assays. Cellular mobility and invasive capacity were detected using wound-healing, Transwell, and cell motility assays. Tumor growth and metastasis were determined using the mouse subcutaneous and pancreatic cancer orthotopic liver metastasis models. The antitumor effects of CLT-003 were evaluated using patient-derived organoid (PDO) and patient-derived xenograft (PDX) models.

Results: CLT-003 significantly inhibited cellular proliferation, enhanced cellular apoptosis, and attenuated cellular invasion and migration of pancreatic cancer cells. Mechanistically, CLT-003 suppressed the translation of HIF-1α by inhibiting the PI3K/AKT/mTOR signaling pathway. In the mouse tumor models, CLT-003 significantly inhibited the growth and metastasis of pancreatic tumors. Moreover, the PDO and PDX models showed increased sensitivity to CLT-003 in pancreatic cancer with high HIF-1α expression compared to pancreatic cancer with low HIF-1α expression.

Conclusions: This study delineated the role and molecular mechanism of CLT-003 action in impeding the progression of pancreatic cancer and indicated its robust potential for the treatment of pancreatic cancer.

KEYWORDS CLT-003; pancreatic ductal adenocarcinoma; HIF-1α; PI3K/AKT/mTOR; malignant progression

Introduction

Pancreatic ductal adenocarcinoma (PDAC) is the leading cause of cancer-related deaths globally with an overall 5-y patient survival rate of approximately 11%[1]. PDAC is predicted to become the second most common cause of death due to cancer by 2030[2]. Most patients are asymptomatic in the early stages of PDAC and progress to advanced stages at the time of diagnosis. The average survival time of patients with PDAC in advanced stages is < 1 y[3]. Chemotherapy can prolong the survival of

*These authors contributed equally to this work.
Correspondence to: Jihui Hao and Xiuchao Wang
E-mail: haojihui@tjmuch.com and wangxiuchao2008@163.com
ORCID ID: https://orcid.org/0000-0001-6966-6730 and https://orcid.org/0000-0002-3205-8544
Received February 10, 2025; accepted July 24, 2025;
published online September 30, 2025.
Available at www.cancerbiomed.org

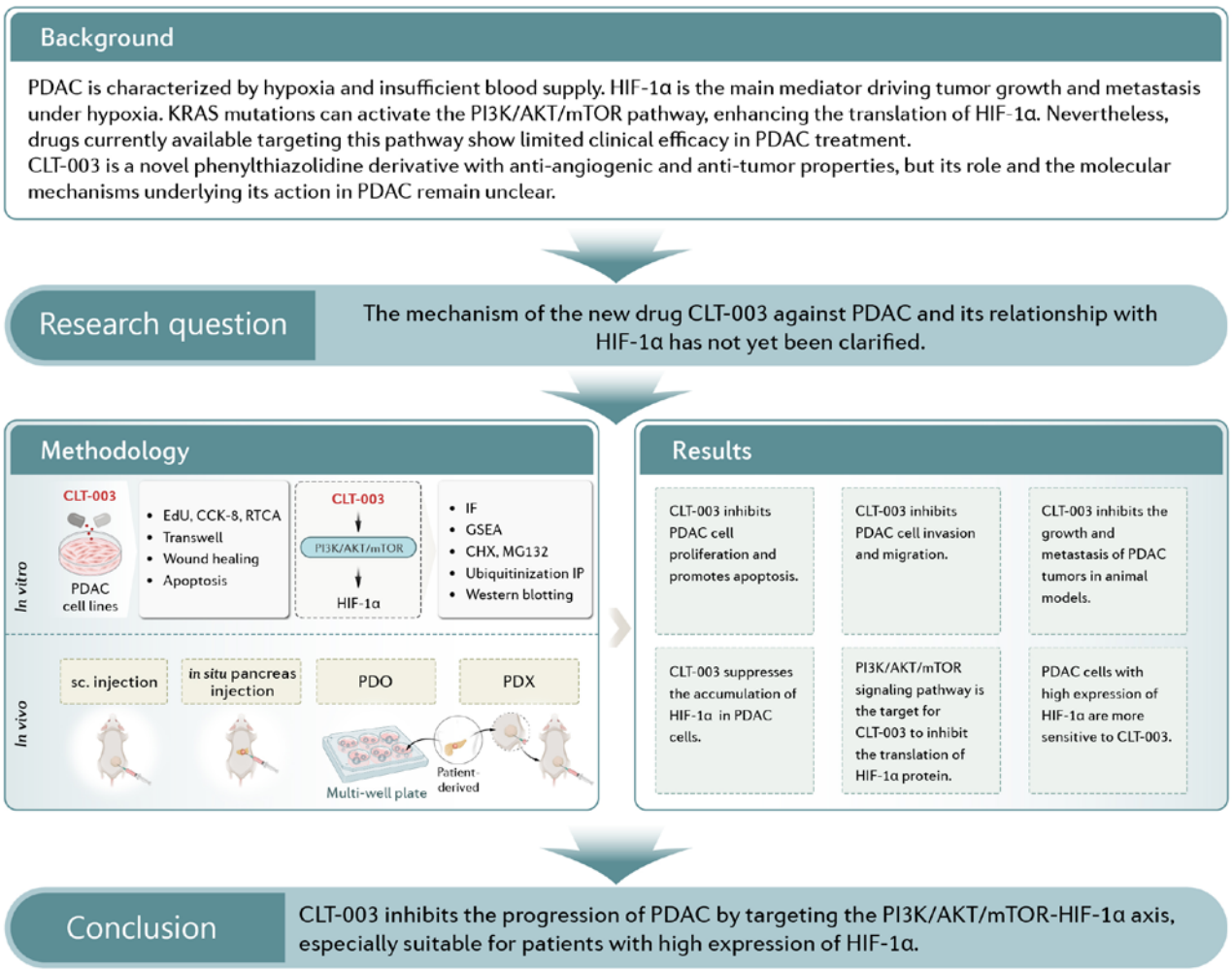

Study flowchart *In vitro*: CLT-003 inhibited PDAC proliferation (EdU/CCK-8/RTCA), migration (Transwell/wound healing), and induced apoptosis. It suppressed HIF-1α protein synthesis via blocking PI3K/AKT/mTOR-mediated translation (validated by MG132/Western blotting), with no significant effect on HIF-1α ubiquitin-proteasomal degradation (CHX chase assays/ubiquitination IP). *In vivo*: CLT-003 reduced tumor growth and metastasis in subcutaneous/pancreatic orthotopic models and patient-derived systems (PDOs/PDXs), showing enhanced efficacy against HIF-1α-high PDAC. Conclusion: CLT-003 selectively targets PI3K/AKT/mTOR-dependent HIF-1α translation to combat PDAC, indicating therapeutic potential for HIF-1α-overexpressing tumors. CCK-8, cell counting kit-8; CHX, cycloheximide; HIF-1α, hypoxia-inducible factor 1-alpha; IF, immunofluorescence; PDAC, pancreatic ductal adenocarcinoma; PDO, patient-derived organoid; PDX, patient-derived xenograft; RTCA, real-time cell analysis.

patients with pancreatic cancer but chemotherapy alone is not the optimal treatment option for pancreatic cancer given the high side effects and drug resistance caused by multiple factors[4]. Hence, more effective medical treatments and drugs are urgently needed to treat patients with pancreatic cancer.

Hypoxia and blood supply deprivation are important features of pancreatic cancer. Hypoxia-inducible factor-1 (HIF-1) is the main mediator of cellular responses to hypoxia[5]. HIF-1 consists of the HIF-1α and HIF-1β subunits. HIF-1α is stabilized and translocated into the nucleus under hypoxic conditions. HIF-1α forms a dimer with HIF-1β and binds to the hypoxia response element (HRE) in the promoter region of downstream genes, thereby activating gene expression and promoting tumor growth and metastases[6]. In previous studies we reported that HIF-1α regulates several genes, including *FSCN1*[7], *LASP1*[8], and *LIMS1*[9], to promote tumor metastasis and adaptation to a hypoxic environment. A series of translational studies targeting HIF-1α were conducted[10-12]. Clinical trials and preclinical studies have shown that targeting HIF-1α is an attractive strategy for treating pancreatic cancer[13].

KRAS mutations, which are present in nearly 90% of PDAC patients, can activate the PI3K/AKT/mTOR pathway and increase the HIF-1α translation rate[14]. Currently, several inhibitors of the PI3K/AKT/mTOR pathway, including alpelisib and duvelisib, have been licensed and marketed for the treatment of lymphoma and breast cancer and show excellent therapeutic effects[15,16]. However, no drug targeting the PI3K/AKT/mTOR pathway is being used in the clinic for pancreatic cancer and the results of some clinical trials are unsatisfactory[17]. Discovering new drugs targeting the PI3K/AKT/mTOR pathway is therefore of great value.

CLT-003 (TC11) [2-(2,6-diisopropylphenyl)-5-amino-1H-isoindole-1,3-dioneis], a novel phenylphthalimide derivative, was encapsulated in poly (lactate-glycolic acid) copolymer nanoparticles using nanotechnology. CLT-003 effectively blocks the increase in VEGF levels in the atrial fluid of diabetic rats and inhibits thickening of the retinal capillary basement membrane[18]. CLT-003 induces apoptosis by degrading MCL1 in multiple myeloma cells and inhibits centrosomal aggregation[19]. However, the role and mechanism of CLT-003 action in pancreatic cancer have not been reported.

In the present study CLT-003 was shown to effectively promote apoptosis and inhibit cell proliferation and metastasis in PDAC cells. CLT-003 exerts these effects mainly by reducing HIF-1α translation by blocking the PI3K/AKT/mTOR pathway. CLT-003 presented a powerful anti-tumor effect in patient-derived organoid (PDO) and patient-derived xenograft (PDX) models that was dependent on HIF-1α inhibition.

Materials and methods

Cell culture

Human PDAC cell lines (SW1990, MIA-PaCa2, CFPAC-1, and BxPC-3), other human tumor-derived cell lines [breast cancer cells (MDA-MB-231), colon cancer cells (SW480), cervical cancer cells (HeLa), and lung cancer cells (A549)], a human embryonic kidney cell line (293T), and a normal human mammary epithelial cell line (MCF-10A) were obtained from American Type Culture Collection [ATCC] (Manassas, VA, USA). None of the cell lines used were contaminated by microorganisms, including *Mycoplasma*. SW1990 and BxPC-3 cells were cultured in RPMI-1640 medium (Gibco, Grand Island, New York, USA). MIA-PaCa2, MDA-MB-231, SW480, HeLa, A549, and 293T cells were cultured in DMEM (Gibco, Grand Island, New York, USA). CFPAC-1 cells were cultured in IMEM (Gibco, Grand Island, New York, USA). MCF-10A cells were cultured in DMEM/F12 (Gibco, Grand Island, New York, USA). All media were supplemented with 10% fetal bovine serum (Vazyme, Nanjing, Jiangsu, China) and 1% penicillin-streptomycin (Solarbio, Beijing, China) and cells were maintained at 37°C in a humidified incubator with 5% CO_2.

Western blotting

Cells were lysed in SDS-NP40 buffer [50 mM Tris (pH 8.0), 150 mM NaCl, 1% NP40, 1% SDS, and 1 mM protease inhibitor cocktail; Beyotime, Shanghai, China] on ice for 1 min. Cells were scraped from the plate and briefly thrice-sonicated. Then, lysates were heated at 95°C for 5 min and centrifuged at 20,000 × g at 4°C for 10 min. Protein lysates (20 μg) were separated by SDS-PAGE and the proteins were transferred onto PVDF membranes (Vazyme, Nanjing, Jiangsu, China). The PVDF membranes were incubated in a blocking buffer (5% non-fat milk in TBST) for 2 h at room temperature (RT). Target proteins were detected by incubation with primary and corresponding secondary antibodies (**Table 1**).

Reverse transcription-polymerase chain reaction (RT-PCR)

Total RNA was isolated from 1×10^6 cells using the TRIzol reagent (Invitrogen, Carlsbad, California, USA) and 1 μg RNA was used for RT-PCR (Takara, city, Japan) analysis. Each RT-PCR sample was assessed in triplicate. Next, the product was used for the subsequent qRT-PCR experiments (Takara, Kusatsu, Shiga, Japan). Transcript abundance was calculated as the difference relative to β-actin levels. The primer sequences for qRT-PCR are listed in **Table 2**.

Immunofluorescence

PDAC cells were seeded on coverslips to evaluate the expression and distribution of HIF-1α under normoxic and hypoxic conditions after CLT-003 treatment and antigen-retrieved sections were obtained. Both groups of cells were incubated with the primary antibody [anti-HIF-1α (1:200)] at

Table 1 Antibodies used in this study

Name	Company	Cat. No.
For WB		
Anti-Bcl-2 antibody	Proteintech	26593-1-AP
Anti-Bax antibody	Proteintech	50599-2-Ig
Anti-HIF-1α antibody	Abcam	ab51608
Anti-p-AKT (thr308) antibody	CST	4056
Anti-AKT antibody	CST	4685
Anti-p-mTOR antibody	CST	2974
Anti-mTOR antibody	Proteintech	28273-1-AP
Anti-p-p70 S6K antibody	CST	9234
Anti-p70 S7K antibody	CST	9202
Anti-VEGFA antibody	Abcam	ab214424
Anti-TGF alpha antibody	Abcam	ab208156
Anti-GLUT1 antibody	Abcam	ab115730
Anti-β-actin antibody	Ray Antibody Biotech	RM2001
For IHC and IF		
Anti-HIF-1α antibody	Abcam	ab51608
Anti-Ki67 antibody	Abcam	ab16667
Anti-capase3 antibody	Proteintech	19677-1-AP

Table 2 Primers and oligonuceotide sequences

qPCR primers	
VEGF	
Forward primer	TTCCAGCAGTTCCCAGAAGGAC
Reverse primer	CCCAGCATTCTTGACAAACCC
GLUT1	
Forward primer	TCTGGCATCAACGCTGTCTT
Reverse primer	CCGTGTTGACGATACCGGAG
TGF-α	
Forward primer	CTCGCTTGGAAGAAATCGCTG
Reverse primer	AGAGAGGGTGTGGAGCTGCTTA

4°C for 16 h and followed by incubation with fluorescent secondary antibodies at RT for 2 h. Cells were mounted with a DAPI nuclear stain (SouthernBiotech, Birmingham, Alabama, USA). The number of positive cells was counted at 40 × magnification in 5 random fields under an Olympus microscope (Shinjuku, Tokyo, Japan).

Animal experiments

SW1990 cells were resuspended in PBS at a density of 10^7 cells/mL to construct subcutaneous tumor models. Five-week-old female nude mice (SPF, Beijing, China) were injected subcutaneously with 100 μL of the SW1990 cell suspension. The mice were administered CLT-003 (50 or 100 mg/kg) or PBS vehicle (Veh.) by intravenous infusion every other day and tumor growth was measured using a caliper every 4 d. Tumors were harvested 4 weeks later. Tumor volume was calculated as follows: volume = 0.5 × length × width × width. Luciferase-labeled SW1990 (SW1990-luc) cells were injected (1×10^6) into the exposed pancreas of 5-week-old female nude mice for orthotopic tumor models. Tumors were analyzed based on bioluminescence imaging (BLI) signals every week.

Four PDX lines with HIF-1α-high or -low expression were used for PDX experiments. PDX tumors were cut into 8 mm^3 pieces and subcutaneously implanted into 5-week-old female NOD/scid mice (SPF, Beijing, China). The same treatment protocol as above was used when the tumor volume reached 50 mm^3. Tumor volume was calculated as follows: volume = 0.5 × length × width × width. Immunochemistry (IHC) staining for Ki67 and caspase-3 was performed to evaluate the proliferation and apoptosis status of tumor tissues. All animal experiments are performed in accordance with the ARRIVE guidelines, the UK Animals (Scientific Procedures) Act 1986 and associated guidelines, and the EU Animal Experimentation Directive 2010/63/EU. The study protocol was reviewed and approved by the Institutional Animal Ethics Committee of Tianjin Medical University Cancer Institute & Hospital (Approval no. AE-2020161).

Organoid culture and experiments

Human PDAC organoid cultures were established and cultured following a previously described protocol[20]. PDAC organoids (1×10^3 cells) wrapped in Matrigel (Corning, New York, USA) were seeded in 96-well plates (cat: CLS3340, Corning, New York, USA) for CLT-003 treatment. The medium was replaced with human complete feeding medium (hCPLT) and CLT-003 (10 μM) after 7 d of culture and incubated for an additional 3 d.

Organoid cell viability detection was monitored by microscopy and measuring the ATP concentrations using Cell Titer-Glo (Promega, Madison, Wisconsin, USA). Patients provided informed consent before participating in the study. This research was approved by the Ethics Committee of

Tianjin Medical University Cancer Hospital (Approval nos. Ek2020155 and bc20252980).

Wound healing and Transwell assays

Wound healing and migration assays were performed using the indicated pancreatic cancer cells, following a previously published protocol[8]. Matrigel was diluted 6-fold and added to the upper chamber of the Boyden cell (Merck, Darmstadt, Hesse, Germany) to assess invasion in the Transwell assay. CLT-003 solutions were prepared in a medium containing 2% fetal bovine serum at concentrations of 0, 2.5, 5, and 10 mM. PDAC cells (5×10^5) were resuspended in the Boyden upper chamber and incubated with various concentrations of CLT-003 solution. The Boyden lower chamber contained medium supplemented with 10% fetal bovine serum and cells were incubated for 12–24 h. The cells that migrated to the bottom of the filter were stained using a three-step staining kit (Thermo Fisher Scientific, Waltham, Massachusetts, USA). A microscope was used for counting and statistical analysis was performed.

5-ethynyl-2′-deoxyuridine (EdU) incorporation assay

Tumor cells were seeded into 96-well plates at a density of 1×10^4 cells per well and cultured overnight in a medium containing CLT-003 at 4°C. EdU (Invitrogen) was added to each well and the cells were incubated at 37°C for 24 h. Detection of EdU was based on a click reaction following immunofluorescence (IF).

Cell apoptosis assay

Cell apoptosis was measured by Annexin V/propidium iodide (PI) staining (BD, Franklin Lakes, New Jersey, USA) following the manufacturer's instructions and subjected to flow cytometry analysis. Tumor cells were grown in a culture medium containing CLT-003 for 48 h.

Automated cell tracking using the Operetta system

Live cell imaging was performed on the Operetta High-content Imaging System (PerkinElmer, Waltham, Massachusetts, USA) equipped with a live cell chamber. The environmental control unit was set to 37°C with 5% CO_2 and images were acquired using an LWD 40X objective in the widefield fluorescence mode. Images were acquired for up to 16 h at intervals of 15 min. Images were segmented using the Find Cells building block of the Harmony software (PerkinElmer, Waltham, Massachusetts, USA), which provides a dedicated algorithm for segmenting digital phase contrast images.

RNA sequencing

SW1990 and MIA-PaCa2 cells were cultured in medium supplemented with fetal bovine serum and antibiotics at 37°C in a 5% CO_2 atmosphere until the cells reached 50% confluence. The cells were divided into two groups (solvent control and CLT-003-treated groups). Ten micromolar CLT-003 was administered to the treated group for 24 h, while the control group received an equal volume of solvent. Following treatment, the medium was aspirated and the cells were rinsed twice with cold PBS. An appropriate amount of Trizol was added to disrupt the cells and mixed thoroughly. The samples were incubated at RT for 5 min. Finally, the samples were collected in RNase-free tubes and sent for sequencing.

Statistical analysis

Statistical analyses were performed using SPSS 18.0 software (IBM, Chicago, Illinois, USA) and GraphPad Prism 9 or version 5.0.3 (GraphPad, San Diego, California, USA). All data are presented as the mean ± SD and repeated at least thrice. All P values < 0.05 were considered statistically significant. $P < 0.05$; *, $P < 0.001$; **, $P < 0.0001$; ***, $P < 0.0001$; ****, $P > 0.05$; ns, not significant.

Results

CLT-003 inhibits PDAC cell proliferation and promotes apoptosis

The chemical structure of CLT-003 is shown in **Figure 1A**. Four human-derived PDAC cell lines (SW1990, MIA-PaCa2, BxPC-3, and CFPAC-1) were treated with different concentrations of CLT-003 to evaluate the effect of CLT-003 on tumor cell growth. CLT-003 exerted a significant inhibitory effect on the proliferation of the PDAC cells (IC_{50} = 2.402 ~ 4.9 μM; **Figure 1B**). CLT-003 also inhibited the proliferation of other cancer cell lines but had a minimal effect on the growth of normal cells [**Figure S1A–F**, breast cancer

(MDA-MB-231) cells, IC_{50} = 6.8 μM; lung cancer (A549) cells, IC_{50} = 3.109 μM; cervical cancer (HeLa cells), IC_{50} = 3.207 μM, and colon cancer (SW480) cells, IC_{50} = 6.808 μM; MCF-10A cells, IC_{50} = 29.5 μM]. Our data also showed that CLT-003 dramatically decreased PDAC cell line colony formation in plates (**Figures 1C, D and S2A, B**). The inhibitory effect of CLT-003 on pancreatic cancer cell proliferation was also dynamically demonstrated by real-time cellular analysis [RTCA] (xCELLigence, Agilent, Santa Clara, California, USA; **Figure 1E, F**). The EdU assay showed that CLT-003 significantly inhibited DNA replication in SW1990 and MIA-PaCa2 cells (**Figures 1G, H and S2C, D**). Flow cytometry assays for SW1990 and MIA-PaCa2 (**Figure 1I, J**) treated with different concentrations of CLT-003 showed that CLT-003 increased the PDAC cell apoptosis rate upon CLT-003 treatment, which was concentration-dependent. Western blot analysis revealed a significant decrease in the expression of the anti-apoptotic protein, Bcl-2, and a significant increase in the expression of the apoptotic protein, Bax (**Figure 1K**), in SW1990 and MIA-PaCa2 cells treated with CLT-003, further demonstrating that CLT-003 promoted apoptosis in PDAC cells. Taken together, the above-mentioned experiments demonstrated that CLT-003 could inhibit cell proliferation and promote apoptosis of PDAC cells *in vitro*.

A subcutaneous transplantation tumor model was established in BALB/c nude mice using SW1990 cells to determine whether CLT-003 can inhibit PDAC tumor growth. Low- (50 mg/kg) or high-dose (100 mg/kg) CLT-003 was administered intravenously every other day beginning on day 7 post-implantation when the short diameter of subcutaneous

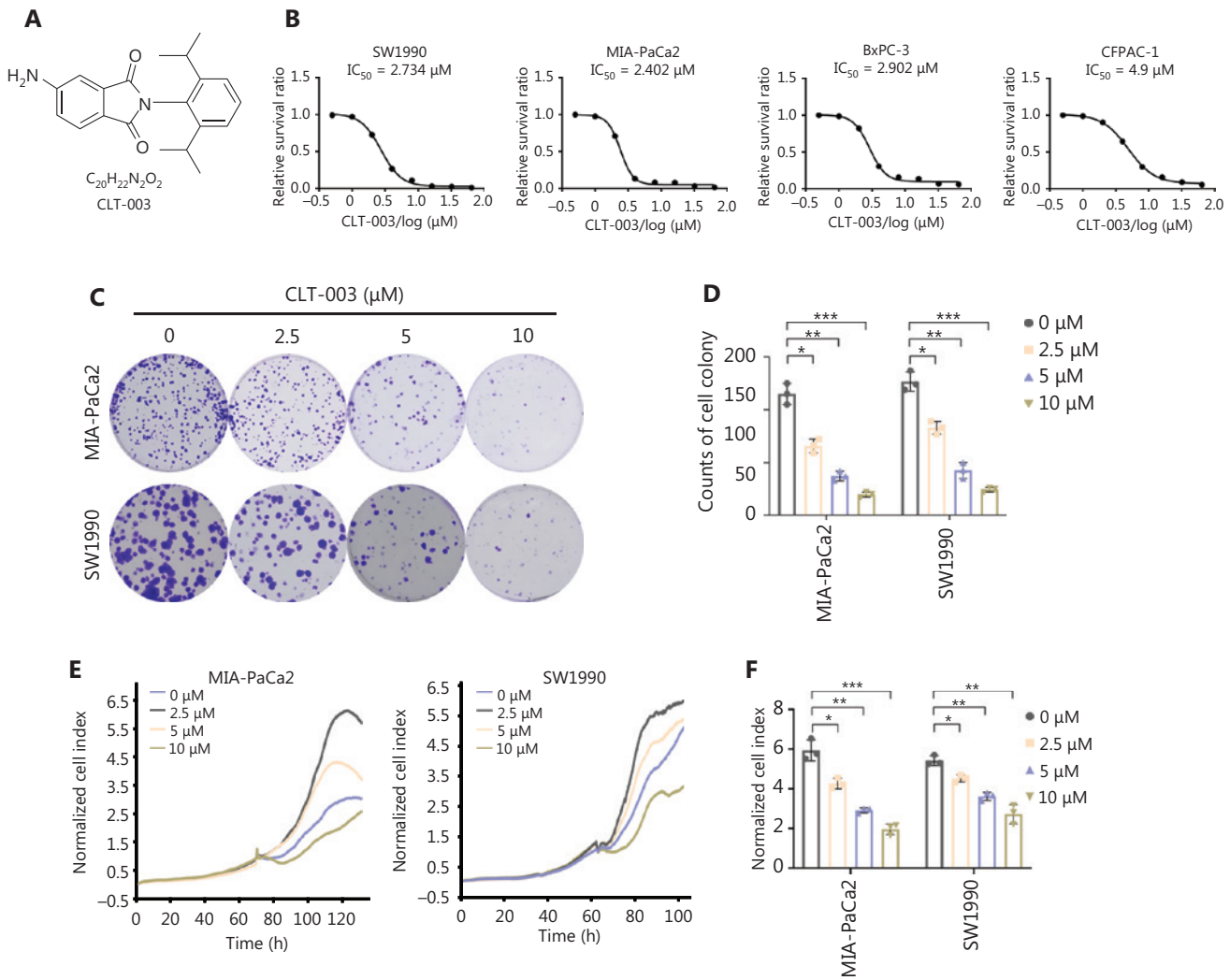

Figure 1 Continued

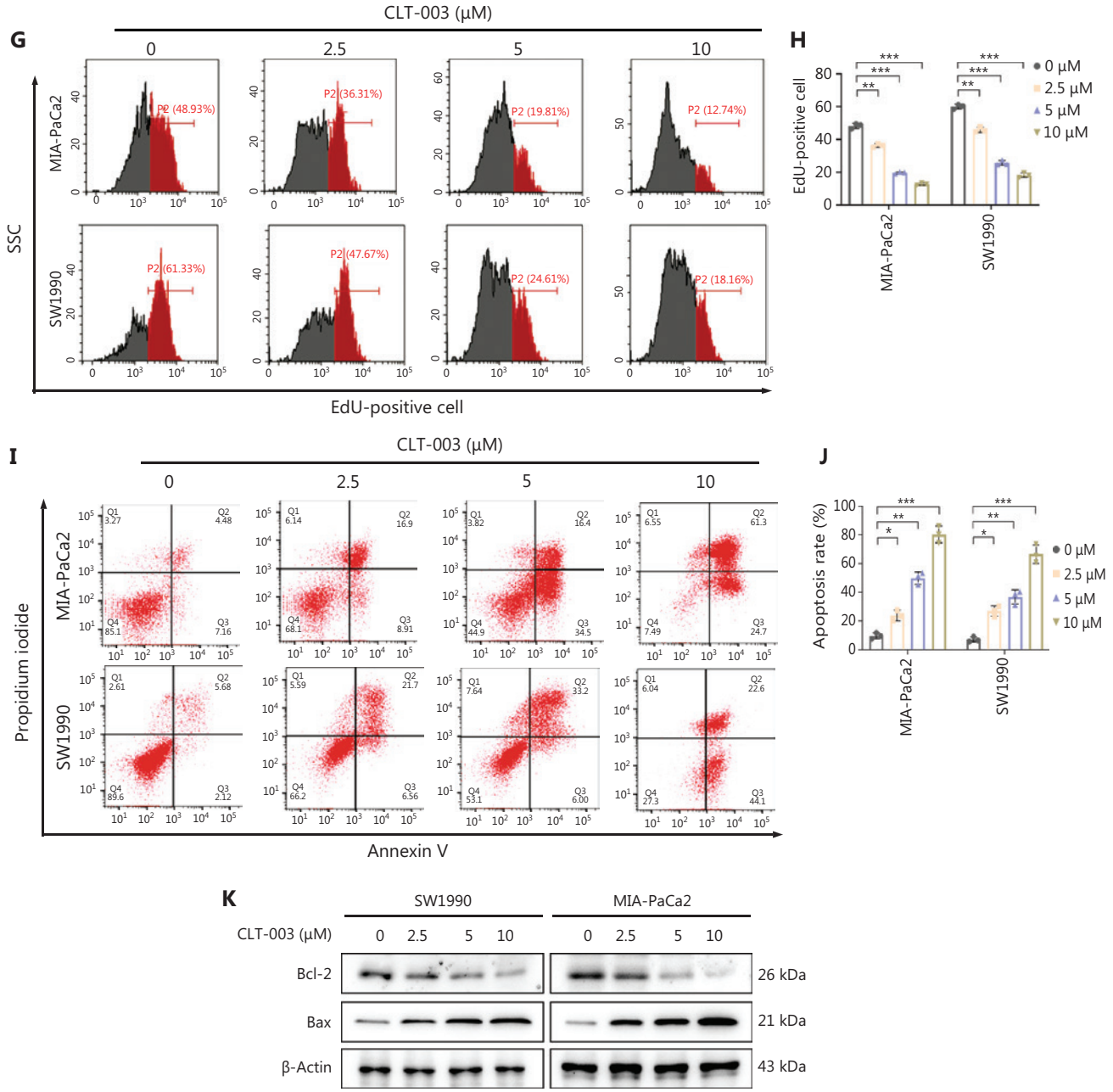

Figure 1 Effects of CLT-003 on the growth and apoptosis of cancer cells. (A) Chemical structure of CLT-003. Molecular formula: $C_{20}H_{22}N_2O_2$. Molecular weight: 322.4 g/mol. (B) CCK-8 assay was performed to detect the cell viability of the indicated pancreatic cancer cell lines (SW1990, MIA-PaCa2, BxPC-3, and CFPAC-1) treated with the indicated concentrations of CLT-003 for 72 h. The values are expressed as the mean deviation of the three independent experiments. (C, D) A colony formation assay (C) was performed using MIA-PaCa2 and SW1990 cell lines following treatment with the indicated concentrations of CLT-003. Bar charts show the colony numbers (D). (E, F) SW1990 and MIA-PaCa2 cells were cultured in a medium containing the indicated concentrations of CLT-003 for real-time cell analysis [RTCA] (xCELLigence) and the curves show the average of three experiments (E). The corresponding 72 h normalized cell index is shown as a histogram (F). (G, H) EdU incorporation assays were performed on MIA-PaCa2 and SW1990 cells after a 24-h treatment with CLT-003 at the indicated concentrations. Representative flow cytometry images (G) and corresponding statistical analyses are shown (H). (I, J) The apoptosis rates of MIA-PaCa2 and SW1990 cells treated with the indicated concentrations of CLT-003 for 12–16 h were determined by flow cytometry (I) and statistical analysis (J). Double staining with Annexin V and PI is shown. (K) The expression of apoptosis-related proteins (Bcl-2 and Bax) was detected by western blotting in SW1990 and MIA-PaCa2 cells treated with the indicated concentrations of CLT-003 for 24 h. Data shown as the mean ± SD in D, F, H, and J, and analyzed using unpaired *t*-tests, *, $P < 0.05$; **, $P < 0.01$; ***, $P < 0.001$.

tumors reached approximately 4–5 mm. The control group received the vehicle solution (**Figure 2A**). Tumor growth and weight change curves were plotted simultaneously. Tumor growth was significantly inhibited in the low- and high-dose CLT-003 treatment groups with the latter being more effective (**Figure 2B, D–F**). There was no significant difference between the groups in terms of body weight (**Figure 2C**) and the proportion of important organs-to-body weight, such as heart, liver, spleen, lungs, and kidneys (**Figure S3A**). Additionally, no significant abnormalities were noted in the HE-stained organs in the CLT-003 group compared to the control group (**Figure S3B**), indicating that CLT-003 had a good biological safety profile. Immunohistochemical staining of tumor sections showed a decrease in Ki67-positivity and an increase in caspase-3 with increasing concentrations of CLT-003, both of which had statistically significant differences (**Figure 2G, H**).

CLT-003 inhibits the invasion and migration of pancreatic cancer cells

Classical wound healing and Transwell assays were performed using different CLT-003 concentrations to treat SW1990 and MIA-PaCa2 cells. The ability of CLT-003-treated cells to migrate and invade were significantly inhibited relative to the control group (**Figure 3A–E**) and this inhibition became more pronounced with increasing concentrations of CLT-003. The same trend also occurred in CFPAC-1 and BxPC-3 cells (**Figure S4A–E**). Next, an automated cell tracking system was used to examine the effects of CLT-003 on cell migration in real-time and dynamically. CLT-003-treated SW1990 and MIA-PaCa2 cells had shorter individual cell displacements compared to control cells (**Figure 3F**), reduced the range of total cell movement (**Figure 3G**), and reduced the average speed (**Figure 3H**).

Next, an orthotopic mouse model of pancreatic tumors was used to determine whether CLT-003 could affect PDAC metastasis. Animals were randomly assigned to a CLT-003 low-dose group (50 mg/kg), a CLT-003 high-dose group (100 mg/kg), and a control group on day 7 of inoculation in an *in situ* BALB/c nude mouse model of a pancreatic tumor when the pancreatic tumor short diameter reached 2–3 mm based on ultrasound measurement (**Figure S5A, B**). Doses of CLT-003 were administered every other day and pancreatic tumors and mouse livers were harvested on day 27 (**Figure 4A**). BLI performed in mice normalized to day 7 on day 27 post-implantation was 3.508 ± 1.170 and 7.547 ± 1.458 in the CLT-003 high- and low-dose groups, respectively, which was significantly lower compared to the control group (BLI = 11.45 ± 2.198, **Figure 4B, C**; $P < 0.0001$ in the high-dose group compared to the control group and $P = 0.0047$ in the low-dose group compared to the control group). The mice were euthanized immediately thereafter and the livers were removed for BLI (**Figure 4D**), which revealed statistically significant lower bioluminescence in the CLT-003-treated group compared to the control group (**Figure 4E**). The number of metastases in the liver surface was determined and the area of liver metastases within the fixed size of the liver HE-stained section was quantified (**Figure 4F–H**). Therefore, CLT-003 significantly inhibited PDAC liver metastases. *In situ* tumors treated with CLT-003 were also significantly smaller compared to controls (**Figure S5C, D**), which was consistent with the results from the subcutaneous tumor model. The survival time was significantly longer in the CLT-003-treated group compared to the control group compared to the *in situ* tumor model, with prolonged survival time being more pronounced in the high-dose CLT-003 group (**Figure 4I, J**). Our data suggested that CLT-003 could inhibit PDAC liver metastases and prolong survival of mice.

CLT-003 inhibited HIF-1α accumulation in PDAC cells

Gene Set Enrichment Analysis (GSEA) of RNA-seq sequencing data suggested a negative correlation between CLT-003 and hypoxia (**Figures 5A and S9**). The key molecule for cellular oxygen perception is HIF-1 and HIF-1α is the central transcription factor. First, CLT-003 did not affect the HIF-1α RNA level, as evidenced by the qRT-PCR experiments (**Figure 5B**). Next, western blotting experiments revealed that CLT-003 inhibited the accumulation of HIF-1α in PDAC cells in a concentration- and time-dependent manner under hypoxic conditions (**Figure 5C–F**). CLT-003 was also confirmed to inhibit the expression of intracellular HIF-1α based on a cellular immunofluorescence assay (**Figure 5G, H**). CLT-003 significantly reduced the mRNA (**Figures 5I and S6A**) and protein expression (**Figure S6B, C**) of *VEGF*, *TGFA*, and *GLUT1*, the downstream target genes of HIF-1, under hypoxic conditions in MIA-PaCa2 and SW1990 cells. Wild-type and HRE mutant plasmids were constructed using the full-length promoter region of VEGF to further investigate whether CLT-003 affected the transcriptional functions of HIF-1α, a classic downstream target gene of HIF-1α, and wild-type and HRE mutant plasmids were transfected into SW1990 or 293T cells.

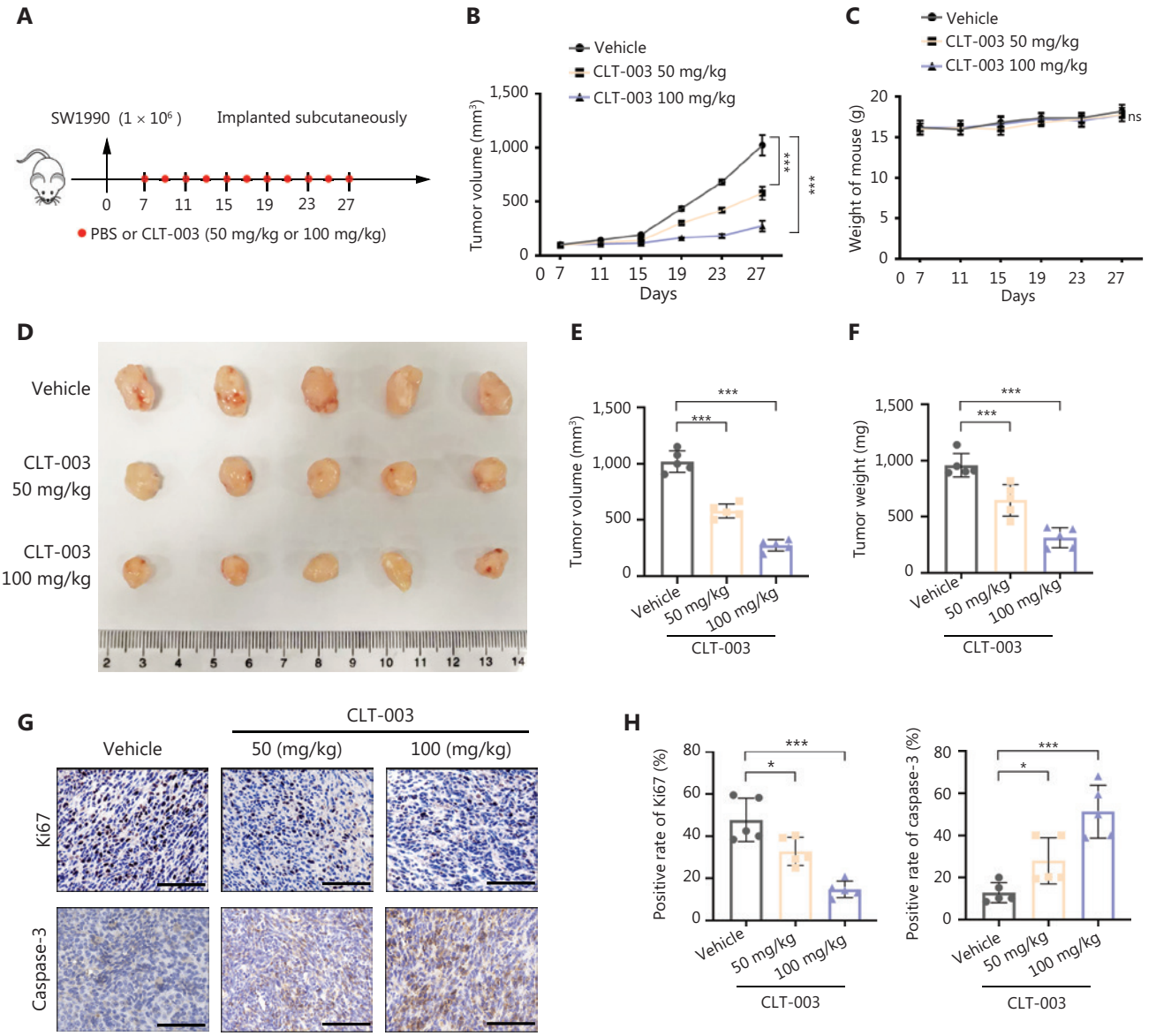

Figure 2 The effect of CLT-003 on the tumor cell growth in mice with pancreatic cancer. (A) SW1990 cells were transplanted into nude mice on day 0 to establish the subcutaneous tumor graft model. CLT-003 (50 mg/kg or 100 mg/kg) or vehicle (red dots indicate the time point of administration) was injected intravenously every other day from day 7 when the short diameter of subcutaneous tumors reached approximately 4–5 mm. (B, C) Tumor volume (B) and the weights of mice (C) were measured every 4 days and plotted. (D–F) Subcutaneous tumors were collected after 3 weeks of treatment with vehicle, low-dose CLT-003 (50 mg/kg), and high-dose CLT-003 (100 mg/kg) (D). Tumor volume (E) and mass (F) were measured and statistically analyzed between groups. (G, H) Representative images of immunohistochemical (IHC) staining for Ki67 and caspase-3 in tumor sections from mice in the vehicle, low-dose CLT-003 (50 mg/kg), and high-dose CLT-003 (100 mg/kg) groups (G). IHC staining results were statistically analyzed (H). Scale bar = 50 μM. Data are shown as the mean ± SD in B, C, E, F, and H, and ANOVA was performed. $P > 0.05$; ns, no significant, *, $P < 0.05$; **, $P < 0.01$; ***, $P < 0.001$.

CLT-003 significantly inhibited the transcriptional activity of HIF-1α in cells transfected with the wild-type VEGF plasmid, as evidenced by the dual luciferase assay (**Figures 5J and S6D**). In conclusion, these results suggested that CLT-003 inhibited the protein accumulation of HIF-1α, resulting in reduced expression of downstream target genes of HIF-1α.

PI3K/AKT/mTOR signaling pathway is the target of CLT-003 to inhibit protein translation of HIF-1α

CLT-003 was shown to exert a non-significant effect on the expression of HIF-1α mRNA but significantly reduced the

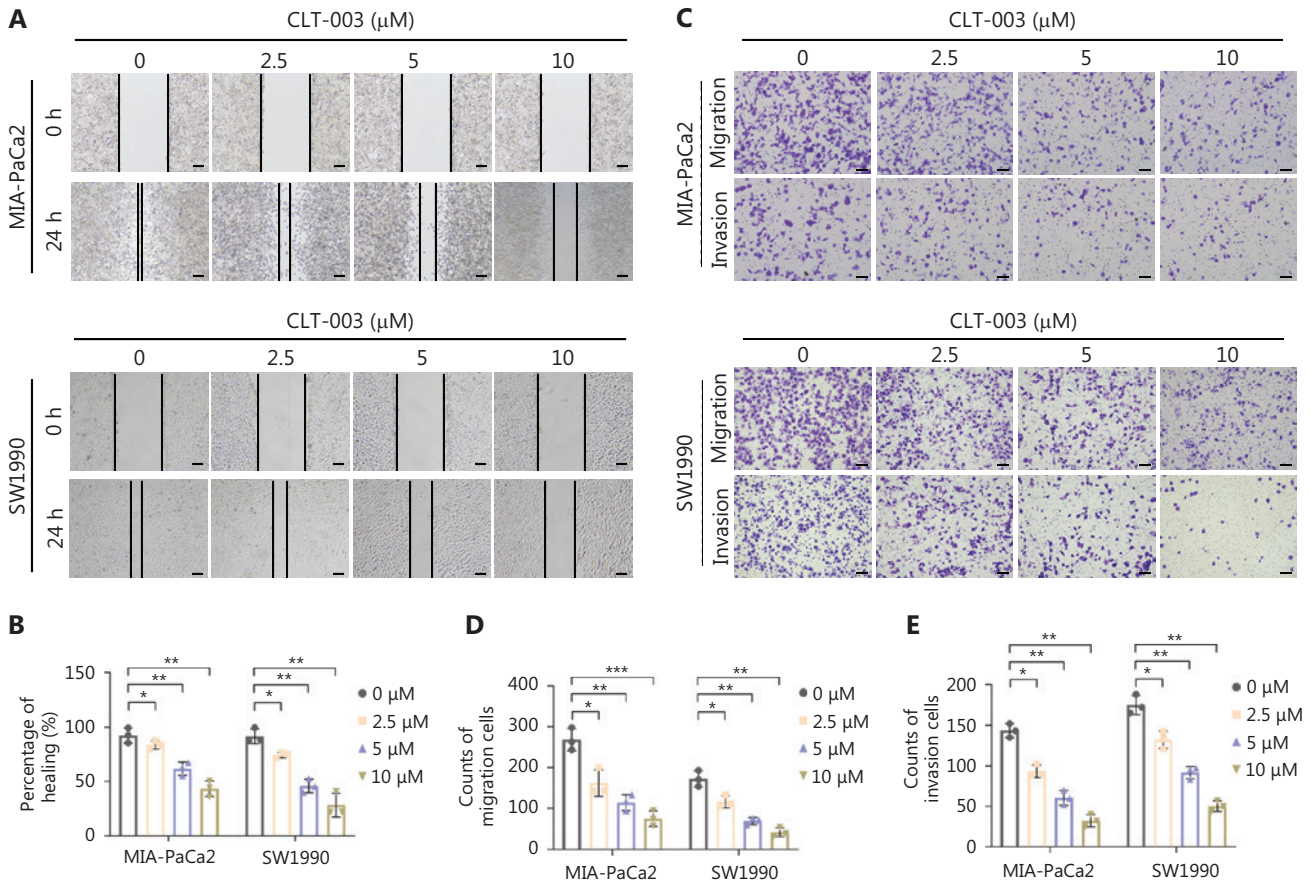

Figure 3 Continued

protein expression of HIF-1α, suggesting that CLT-003 affects HIF-1α protein expression mainly by post-transcriptional regulation[21]. Post-transcriptional HIF-1α protein expression is mainly influenced by translational synthesis and post-translational ubiquitination-mediated degradation. Therefore, whether CLT-003 inhibited HIF-1α protein expression separately was determined. Activation of the PI3K/AKT/mTOR signaling pathway has been reported to promote the translation of HIF-1α protein under hypoxic conditions[22]. Previous research by our group demonstrated that activation of the AKT/mTOR signaling pathway promotes HIF-1α protein translation, thereby regulating HIF-1α protein expression without affecting mRNA levels[9]. Previous studies have reported that various HIF-1α inhibitors suppress HIF-1α expression by inhibiting the AKT/mTOR signaling pathway and subsequently blocking HIF-1α translation[23-25]. Therefore, the effect of CLT-003 on P70 S6K, mTOR, and AKT, the key molecules of the PI3K/AKT/mTOR signaling pathway in pancreatic cancer cells, was determined by western blot analysis. The expression of p-P70 S6K, p-mTOR, and p-AKT (Thr308) was significantly reduced in CLT-003-treated cells compared to the control group under hypoxic conditions (**Figures 6A and S7A**). CLT-003 effects on ubiquitin-mediated HIF-1α degradation and the post-blockade influence on HI F-1α expression were evaluated using three complementary approaches [protein degradation assays, ubiquitination immunoprecipitation (IP), and MG132 chase experiments]. CLT-003 treatment showed no significant difference in HIF-1α degradation kinetics compared to controls following inhibition of *de novo* protein synthesis (**Figures 6B, C**, **S7B, C, and S10**). Ubiquitination levels of HIF-1α remained unaltered independent of CLT-003 treatment (**Figures 6D and S7D**), indicating negligible effects on post-translational ubiquitin-dependent degradation. CLT-003 persistently suppressed HIF-1α expression, even upon proteasomal inhibition by MG132 (**Figures 6E and S7E**). Collectively, these findings demonstrate that CLT-003 modulates HIF-1α expression by inhibiting the PI3K/AKT/mTOR pathway, attenuating HIF-1α mRNA translation (**Figure 7**).

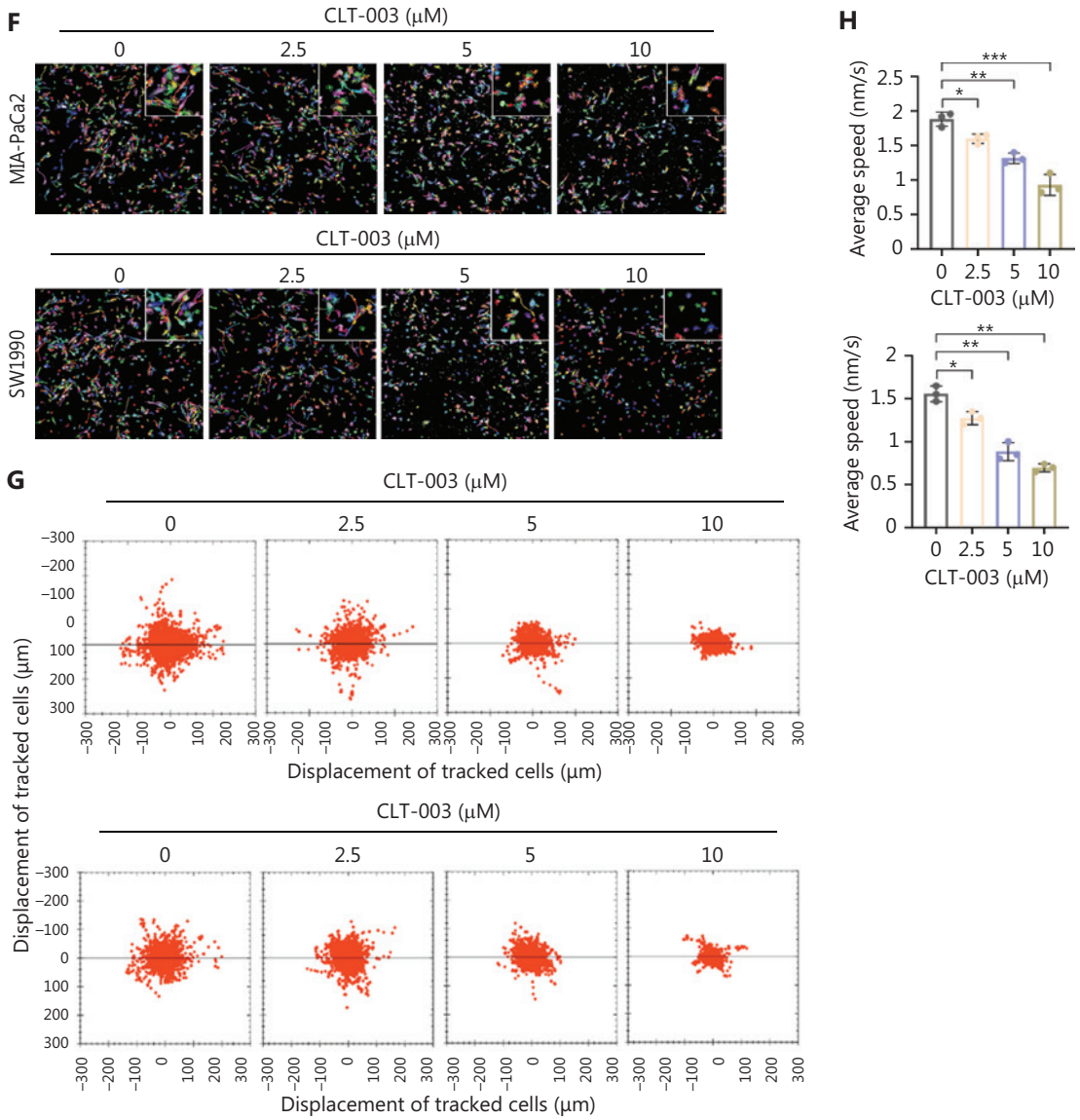

Figure 3 Effect of CLT-003 on the invasion and migration of PDAC cancer cells. (A, B) Wound healing experiment (A) was performed in MIA-PaCa2 and SW1990 cells treated with the indicated concentrations of CLT-003. The percentage of wound healing after 24 h was statistically analyzed (B). Scale bar = 100 μM. (C–E) Transwell assays (C) were performed using MIA-PaCa2 and SW1990 cells treated with the indicated concentrations of CLT-003 for 12–18 h to assess and statistically analyze their migratory (D) and invasive abilities (E). Scale bar = 50 μM. (F–H) Dynamic imaging analysis of cell migration. Cells were pretreated with the indicated concentrations of CLT-003 for 24 h. Cell migration was tracked on automated cell tracking system for > 18 h. Representative images of single-cell movement trajectories (F) and cell limit displacement (G) are shown. The average speed measurement is shown in (H). Data in B, D, E, and H are shown as the mean ± SD and analyzed using an unpaired *t*-test. *, $P < 0.05$; **, $P < 0.01$; ***, $P < 0.001$.

HIF-1α-high PDAC cells are more sensitive to CLT-003

We selected three HIF-1α-high and three HIF-1α-low PDAC patients to establish PDO models (**Figure S8A**) and tested the sensitivity to CLT-003. As shown in **Figure 8A, B**, the inhibition rate following CLT-003 treatment (10 μM) on HIF-1α-low and -high PDOs was 25.78 ± 6.54% and 88.33 ± 9.21%, respectively, suggesting that PDAC patients with high expression of HIF-1α may be more sensitive to CLT-003 treatment. Following the induction of HIF-1α overexpression in HIF-1α-low-expressing PDOs (**Figure S8B**),

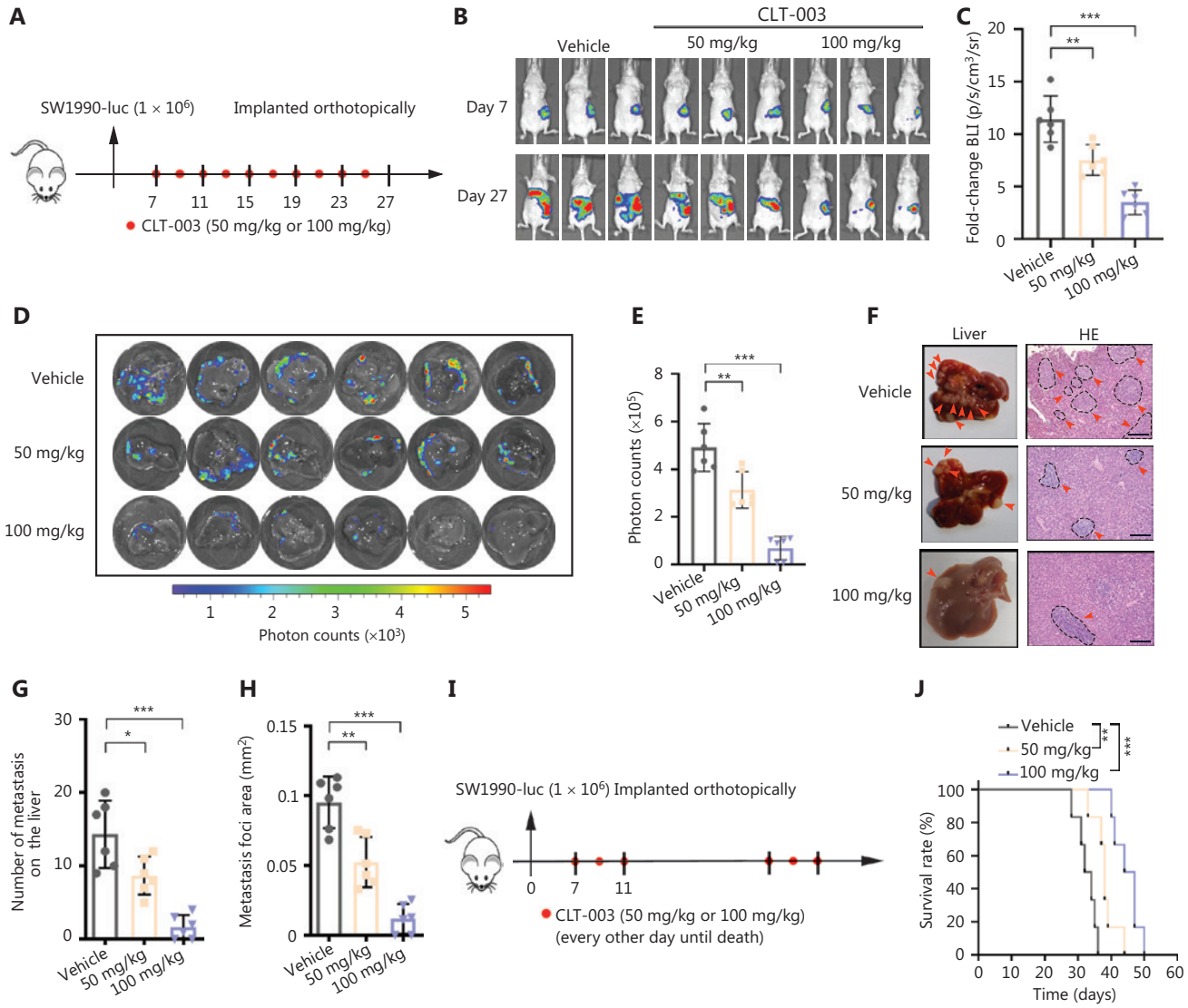

Figure 4 The effect of CLT-003 on pancreatic cancer cell metastasis. (A) The pancreas of BALB/c nude mice was orthotopically injected with 1 × 10^6 luciferase-expressing SW1990 cells (SW1990-luc) in Matrigel. CLT-003 (50 mg/kg or 100 mg/kg) or vehicle was administered intravenously every other day (red dots indicate dosing time points) from day 7 when pancreatic tumor short diameter reached 2–3 mm by ultrasound. (B, C) Bioluminescence imaging (BLI) was performed to assess the growth of SW1990-luc xenografts in the pancreas of mice in the three groups. Representative BLI (B) on days 7 and 27 of tumor implantation. Statistical analysis (C) of the fold change in BLI after treatment (BLI on day 27 compared to BLI on day 7). (D, E) *Ex vivo* BLI (D) of livers extracted from nude mice on day 27 after pancreatic orthotopic implantation. BLI data of liver metastases were quantified (E). (F) Anatomic images of the liver in the three groups. Hematoxylin-eosin (HE) staining confirmed liver metastases. Red arrows indicate metastases on the liver surface and in HE images. Scale bar = 100 μM. (G, H) Statistical analysis of the total number of visible metastatic lesions on the liver surface and metastases foci in the liver were analyzed by ANOVA. (I) The pancreas of BALB/c nude mice was orthotopically injected with 1 × 10^6 SW1990-luc cells in Matrigel. CLT-003 (50 mg/kg or 100 mg/kg) or vehicle was administered intravenously every other day until death (red dots indicate dosing time points) from day 7. (J) Kaplan-Meier survival curves and log-rank tests for significance assessment between control and CLT-003 treatment groups. n = 6, P < 0.01; **, P < 0.001; ***. Data in C, E, G, and H are shown as the mean ± SD using ANOVA analysis. *, P < 0.05; **, P < 0.01; ***, P < 0.001.

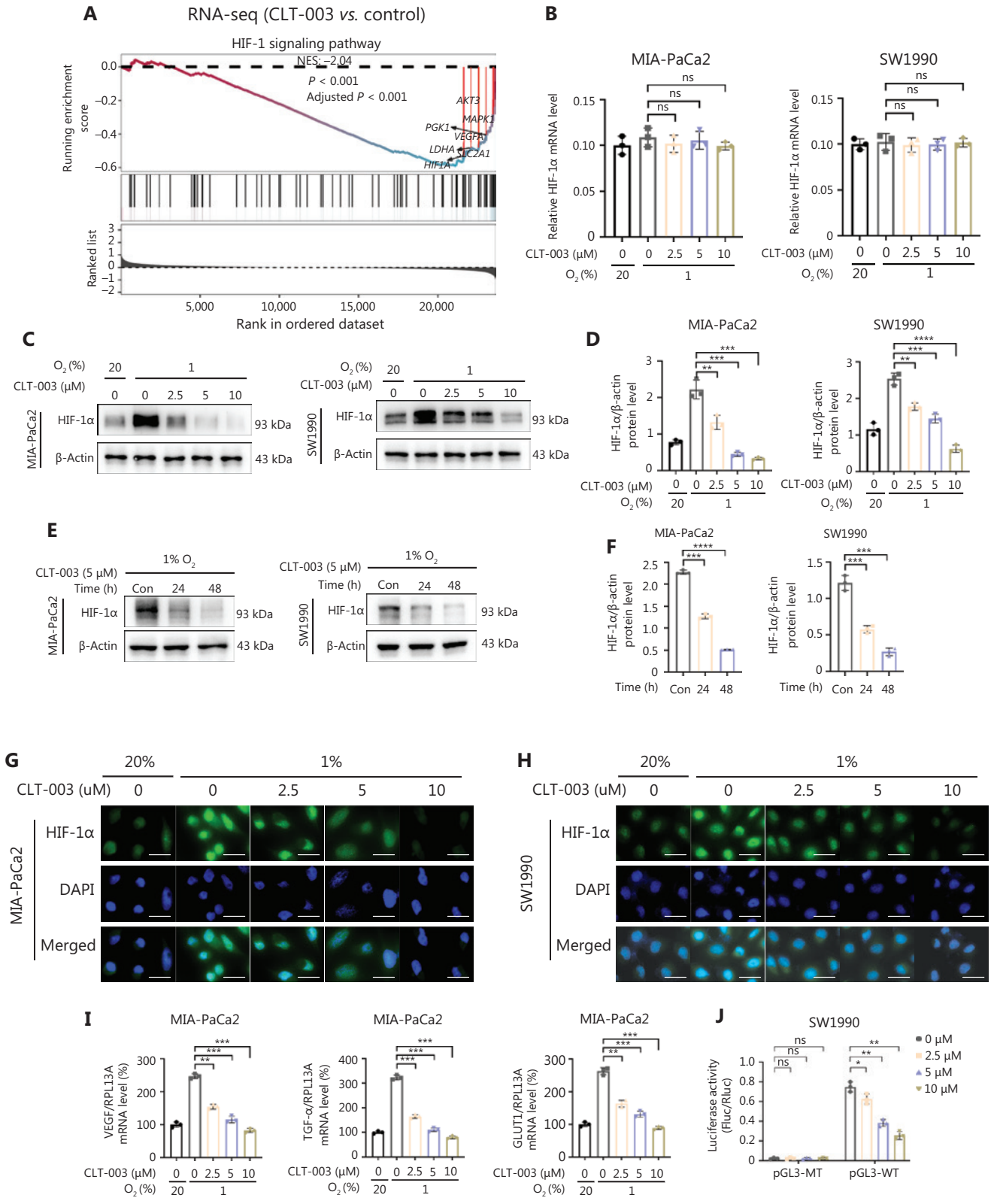

Figure 5 Continued

Figure 5 CLT-003 inhibits HIF-1α accumulation in PDAC cells. (A) GSEA of RNA sequencing data from SW1990 cell lines untreated or treated with CLT-003 (10 μM, 24 h). The relationship between CLT-003 treatment and hypoxia. NES = −2.04, $P < 0.001$. (B) qRT-PCR analysis of mRNA levels of HIF-1α in MIA-PaCa2 and SW1990 cell lines treated with the indicated concentrations of CLT-003 under hypoxic conditions. (C, D) The expression of HIF-1α protein in MIA-PaCa2 and SW1990 cells treated with the indicated concentrations of CLT-003 under hypoxic conditions was detected by western blotting (C). Statistical analysis of gray-scale values of HIF-1α protein expression (D). (E, F) The changes in HIF-1α protein expression in MIA-PaCa2 and SW1990 cells under hypoxic conditions treated with CLT-003 (5 μM) for 24 and 48 h were detected by western blotting (E). Statistical analysis plots of gray-scale values of HIF-1α protein expression (F). (G, H) Immunofluorescence staining of HIF-1α in MIA-PaCa2 and SW1990 cells treated with the indicated concentrations of CLT-003. Scale bar = 20 μM. (I) qRT-PCR analysis was performed to detect the mRNA expression of HIF-1α target genes (*VEGF*, *TGFA*, and *GLUT1*) in MIA-PaCa2 cells treated with the indicated concentrations of CLT-003. (J) Under hypoxic conditions, SW1990 cells were transiently transfected with the full-length plasmid of the wild-type VEGF promoter region and the plasmid with the mutated VEGF promoter region of the HRE region followed by treatment with the indicated concentrations of CLT-003 for 24 h. The transcriptional activity of VEGF was detected and statistical analysis was performed. Data are shown as the mean ± SD in B, D, F, I, and J, and unpaired *t*-tests were performed shown in B, I, and J and paired *t*-tests in D and F. $P > 0.05$; ns, no significant, *, $P < 0.05$; **, $P < 0.01$; ***, $P < 0.001$; ****, $P < 0.0001$.

the inhibitory effect of CLT-003 was more profound, demonstrating stronger efficacy of the compound in HIF-1α-elevated experimental models (**Figure 8C, D**). To validate this finding, PDX tumors from two HIF-1α-high PDAC patients (patients 211 and 139) and two HIF-1α-low PDAC patients (patients 203 and 180) were implanted into NSG mice (**Figure S8C**). When the tumors had a volume of approximately 50 mm^3, the mice were treated with control or CLT-003 (100 mg/kg) for 45 days. The inhibition rate of CLT-003 treatment on two HIF-1α-high PDX tumors was 73.4 ± 2.054% (PDX-211) and 79.83 ± 3.783% (PDX-139; **Figure 8E**). In contrast, CLT-003 inhibited the growth of HIF-1α low-expressing PDX tumors by 11.56 ± 4.726% (PDX-203) and 22.44 ± 6.146% (PDX-180; **Figure 8F**). The expression of Ki67 was significantly reduced in HIF-1α-high PDX tumor tissues after CLT-003 treatment, while caspase-3 staining was significantly elevated (**Figures 8G, H and S8D–G**). To determine whether HIF-1α was a key target for the antitumor effect of CLT-003, HIF-1α was knocked down using the CRISPR/Cas9 technique in a cell line derived from HIF-1α-high PDX-211 (**Figure S8H**). HIF-1α KO abolished the antitumor effect of CLT-003 treatment (100 mg/kg) in the HIF-1α-high PDX line (**Figures 8I, J and S8I**), suggesting that CLT-003 sensitivity required HIF-1α. In summary, PDAC cells with high expression of HIF-1α were more sensitive to CLT-003 inhibition than tumors with low expression of HIF-1α. HIF-1α-high expression in pancreatic cancer could serve as a therapeutic target of CLT-003 to inhibit tumor growth and prevent metastases.

Discussion

As a critical regulator of pancreatic cancer in response to the hypoxic microenvironment, HIF-1 targets the transcription of multiple downstream genes, including *GLUT1*, *TGFA*, and *VEGF*, and is implicated in tumor cell proliferation, invasion, metastasis, and angiogenesis, all eventually leading to poor survival[26]. PDAC cells expressing activated KRAS modulate tumor cell glycolysis by stabilizing HIF-1α expression, resulting in tumor proliferation and metastases[14]. Overexpression of HIF-1α is associated with abnormal p53 accumulation and promotes the progression of pancreatic cancer by activating downstream signaling pathways[27]. Several clinical trials and preclinical studies have shown that targeting HIF-1α is an effective strategy for the treatment of pancreatic cancer[13,28]. Therefore, various strategies have been developed to inhibit pancreatic cancer cell proliferation and metastases by inhibiting HIF-1α[23].

Several compounds have been identified as functional inhibitors of HIF-1 that reduce the level of HIF-1α expression[29]. Monoclonal antibodies are effective in targeting cell surface or soluble antigens but less effective in targeting intracellular components given the high molecular weight[30]. RNA interference technology has been used for downregulating HIF-1α but instability and inefficiency limit application[31]. The CRISPR/Cas9 system is an effective method for silencing oncogenes. However, the off-target effect limits further clinical application[32]. Small-molecule inhibitors have the following advantages: low molecular weight; easier penetration in tumor tissues and direct action on cancer

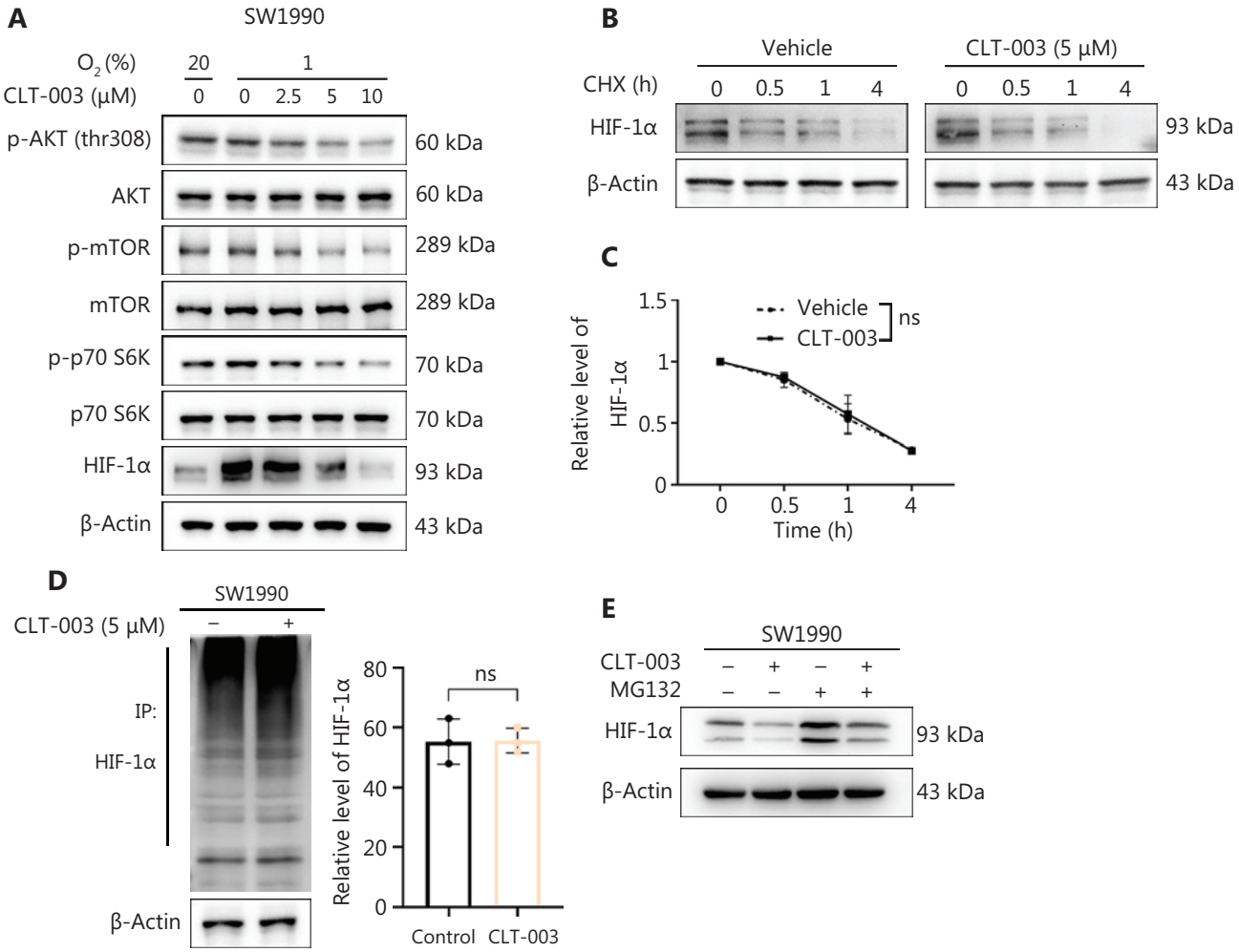

Figure 6 CLT-003 inhibits the protein translation of HIF-1α in pancreatic cancer cells. (A) Western blotting was performed to detect key proteins and phosphorylation in the PI3K/AKT/mTOR pathway in SW1990 treated with the indicated concentrations of CLT-003. (B) SW1990 cells were treated with blank solvent and CLT-003 5 μM/L for 24 h under normoxic conditions, followed by the addition of cycloheximide (CHX, 100 μg/mL) to inhibit protein synthesis. The proteins were extracted from each group after 30 min, 1 h, 2 h, and 4 h, as indicated. The levels of HIF-1α protein expression at the indicated time points were determined by western blot analysis. (C) The gray-scale values of HIF-1α were quantified after normalization to the levels of β-actin using Image J. Data are shown as the mean ± SD and ANOVA was performed. $P > 0.05$; ns, no significant. (D) HIF-1α was immunoprecipitated and analyzed by western blotting to detect ubiquitylated HIF-1α in the vehicle and CLT-003-treated group using an anti-ubiquitin antibody. SW1990 cells were treated with vehicle or CLT-003 5 μM for 24 h under normoxic conditions, then treated by MG132 (1 μg/mL) for 6 h prior to harvesting. Statistical plot based on the grey scale values of ubiquitinated HIF-1α using Image J using paired *t*-tests. Data are shown as the mean ± SD. $P > 0.05$; ns, no significant. (E) SW1990 were incubated for 24 h without, alone, or simultaneously with 10 nM MG132 and 5 uM CLT-003. Western blotting was performed to detect the level of HIF-1α.

cells; easier transport across cell membranes and targeting intracellular components; and high effectiveness when taken orally. Therefore, small-molecule inhibitors are widely used in the treatment of tumors[33].

The PI3K/AKT/mTOR signaling pathway, a growth factor-mediated cascade, represents the major pathway for HIF-1α translation in > 70% of human cancer cell lines[34]. Multiple inhibitors (RAD001[35], HS-116[36], HS-106[37], IPD-196[38], and YC-1[39]) significantly suppress HIF-1α expression across diverse cancer types by targeting the PI3K/AKT/mTOR signaling pathway with inhibition rates > 90% in specific tumor models. PI3K/AKT/mTOR activation can increase the translation rate, leading to increased expression of HIF-1α[34]. LY294002 and wortmannin, PI3K-specific inhibitors,

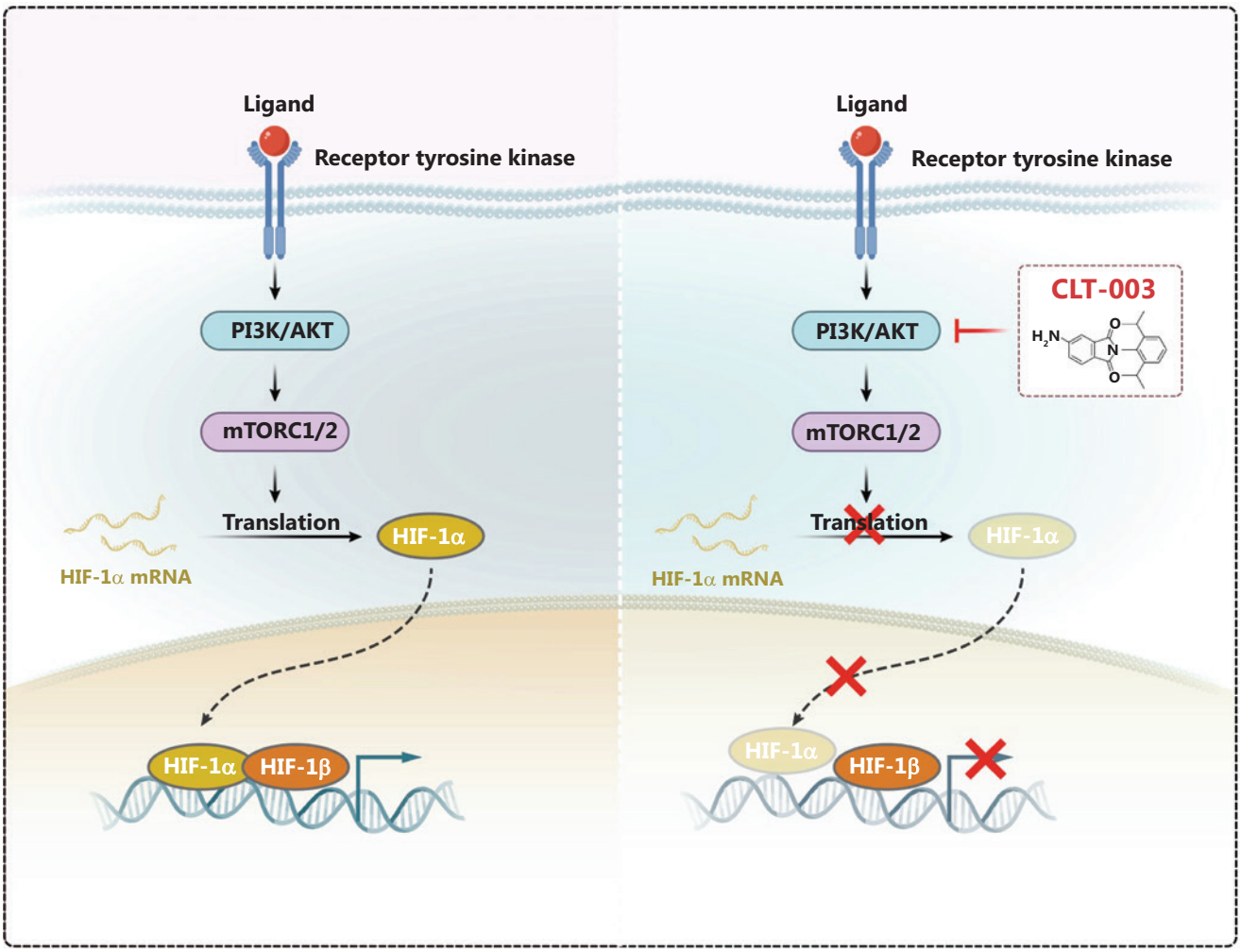

Figure 7 Schematic representation of CLT-003 inhibition of HIF-1α translation by blocking the PI3K/AKT/mTOR axis. (Left panel) In the absence of CLT-003, activation of the receptor tyrosine kinase by a ligand leads to the activation of PI3K/AKT, which in turn activates mTORC1/2. This activation promotes the translation of HIF-1α mRNA into HIF-1α protein, which then dimerizes with HIF-1β to form the active HIF-1 complex, initiating transcription of target genes. (Right panel) In the presence of CLT-003, the CLT-003 inhibits the PI3K/AKT pathway, thereby blocking the activation of mTORC1/2. This inhibition prevents the translation of HIF-1α mRNA, reducing the levels of HIF-1α protein and consequently the formation of the active HIF-1 complex, which leads to decreased transcription of target genes. PI3K, phosphatidylinositol-4,5-bisphosphate 3-kinase; AKT, protein kinase B; mTOR, mammalian target of rapamycin; HIF; hypoxia-inducible factor; black arrows indicate pathway activation and red cross indicates pathway inhibition.

can inhibit HIF-1α protein synthesis in prostate cancer cells (PC-3 and Du145) in a dose-dependent manner[40]. Herein, we introduced a new small chemical molecule that effectively inhibited PI3K/AKT/mTOR pathway activation and reduced HIF-1α expression. CLT-003 had minor effects on HIF-1α mRNA levels but significantly reduced protein expression in a dose-dependent fashion. Moreover, CLT-003 had no apparent effect on the ubiquitination-mediated degradation of HIF-1α but significantly inhibited the activity of the PI3K/AKT/mTOR pathway and reduced the level of HIF-1α protein during translation, resulting in the downregulation of HIF-1α-targeted genes, including *VEGF*, *TGFA*, and *GLUT1*. This finding is consistent with the report presented at the 2009 ARVO Annual Meeting that showed CLT-003 attenuated HIF-1 activation and inhibited angiogenesis in cases of diabetic macular edema[41].

CLT-003 has been previously reported to be effective in treating multiple myeloma, primarily by degrading MCL1

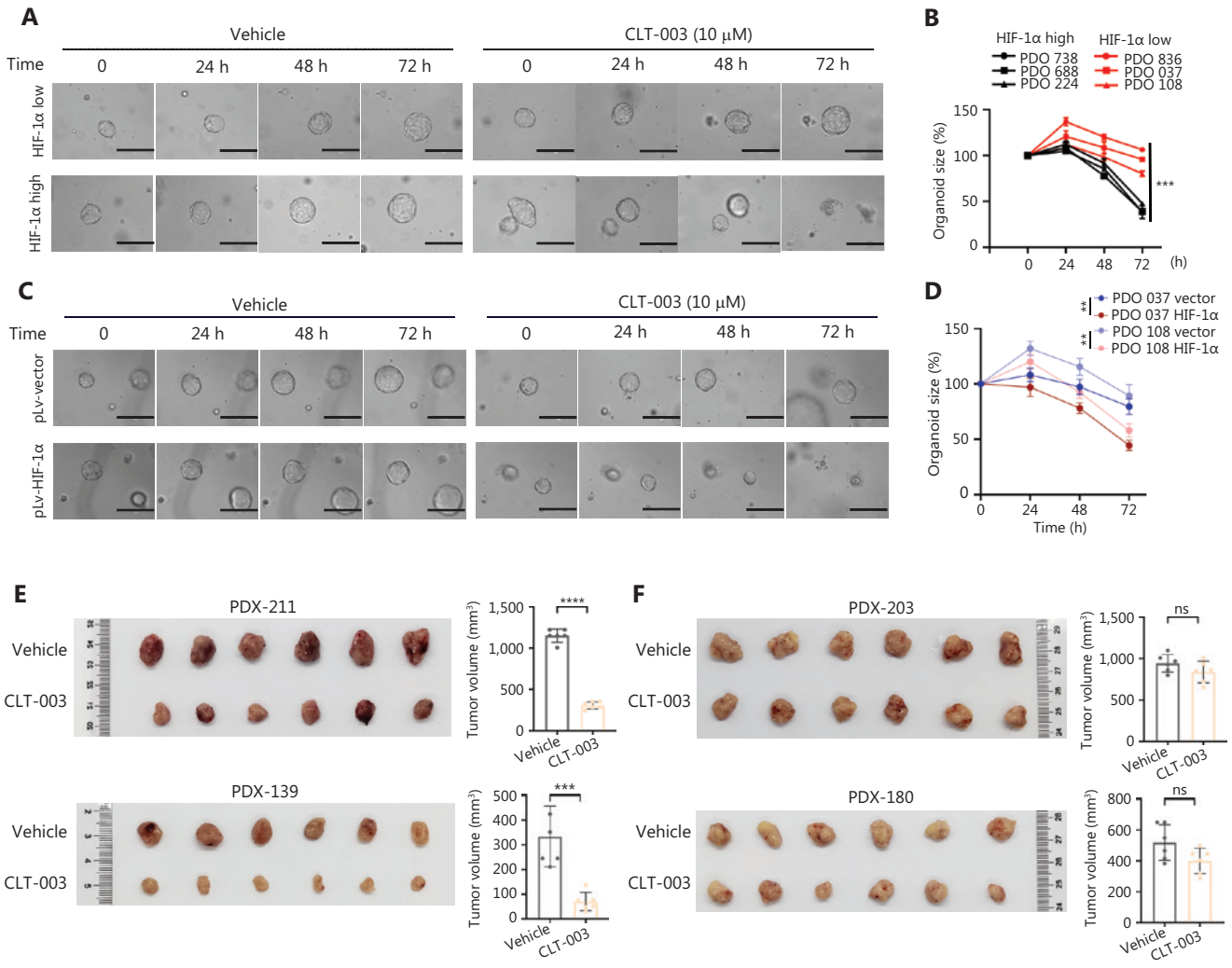

Figure 8 Continued

and activating caspase-9 and CDK1 to promote apoptosis[19]. However, whether CLT-003 is effective in treating pancreatic cancer remains largely unclear due to scarce evidence. Our study showed that CLT-003 remarkably restrained pancreatic cancer cell proliferation and facilitated apoptosis *in vitro*. In addition, CLT-003 effectively inhibited the invasion and migration of PDAC cells and attenuated motility. These findings were verified in subcutaneous tumorigenesis and *in situ* pancreatic tumorigenesis mouse models. PDO and PDX models with high HIF-1α expression were sensitive to CLT-003 treatment. In contrast, PDX cells showed no sensitivity toward CLT-003 treatment after knocking down HIF-1α, indicating that the inhibitory effect of CLT-003 on pancreatic cancer was mainly dependent on inhibition of HIF-1α expression.

The IC_{50} of CLT-003 was > 2 μM in pancreatic cancer and other cancer cell lines. Greater than 50 mg of CLT-003 was administered to mice. However, CLT-003 showed a satisfactory biological safety profile without significant impact on normal cell growth, as well as on the body weight and vital organs of the mice. HIF 1 and 2α (HIF1A and HIF2A) are involved in tumor immune escape mechanisms[42]. All the animal experiments in this study were performed in nude mice, excluding the effect of immunity on tumors. The effects of CLT-003 on the tumor microenvironment and immunity warrant follow-up studies.

In conclusion, our results suggested that CLT-003 is a potent inhibitor of HIF-1α and acts by inhibiting the PI3K/AKT/mTOR signaling axis. Accordingly, CLT-003 exhibited greater efficacy in PDAC patients with high HIF-1α

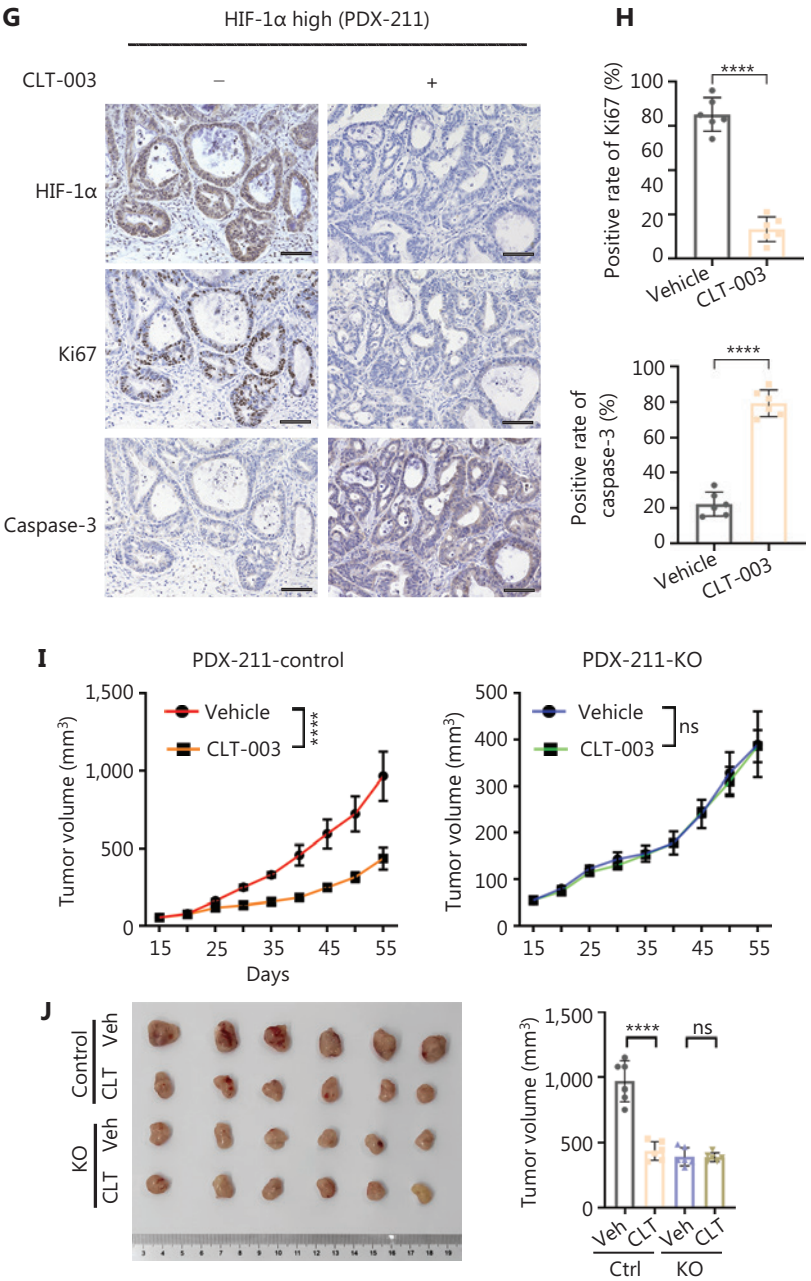

Figure 8 HIF-1α-high PDAC was more sensitive to CLT-003 in patient-derived organoid (PDO) and PDX models. (A, B) The effect of CLT-003 (10 μM) on the growth of PDOs obtained from HIF-1α-high (PDO 738, PDO 688, and PDO 224) or HIF-1α-low PDAC patients (PDO 836, PDO 037, and PDO 108) is shown as representative bright-field micrographs (A) or quantification of PDO growth over time (B). Scale bar = 400 μm. (C, D) The effects of CLT-003 (10 μM) on the growth of PDOs obtained from two HIF-1α-low PDAC patients (PDO 037 and PDO 108), which were transfected with pLv-Vector or pLv-HIF-1A, are illustrated by representative brightfield micrographs (C) or quantification of PDO growth over time (D). Scale bar = 400 μm. (E, F) Tumor anatomy (left) and volume statistics (right) for the effect of CLT-003 administration on tumor growth in PDX with high HIF-1α (PDX-211 and PDX-139) or low HIF-1α (PDX-203 and PDX-180), n = 6. (G, H) Representative IHC staining images for HIF-1α, Ki67, and caspase-3 in PDX-211 (G) and statistical analysis (H) of the immunohistochemical scores of Ki67 and caspase-3 staining from experimentally harvested PDX tumors in E. Scale bar = 100 μm. (I, J) The difference in the efficacy of CLT-003 on HIF-1α-high PDX-211 treatment post-HIF-1α KO is shown in the tumor volume growth curve (I) and the harvested tumor volume at the end of the experiment (J). Data are shown as the mean ± SD in B, D, E, F, H, J, and were analyzed using ANOVA. $P > 0.05$; ns, no significant, **, $P < 0.01$; ***, $P < 0.001$; ****, $P < 0.0001$.

expression. These preclinical data provide a theoretical basis for the development and use of CLT-003 for the treatment of PDAC patients.

Acknowledgments

We would like to thank all the students, colleagues, and teachers who assisted in the completion of the project.

Grant support

This work was supported by the National Natural Science Foundation of China (Grant Nos. 82472973, 82030092, 82273362, 82272680, and 82103006), the National Key Research and Development Program of China (Grant No. 2021YFA1201100), the Tianjin Natural Science Foundation (Grant Nos. 19JCJQJC63100 and 22JCQNJC00100), the Science & Technology Development Fund of Tianjin Education Commission for Higher Education (Grant No. 2022KJ221), and the Tianjin Key Medical Discipline (Specialty) Construction Project (Grant No. TJYXZDXK-009A).

Conflict of interest statement

No potential conflicts of interest are disclosed.

Author contributions

Conceived and designed the analysis: Xiuchao Wang, Jihui hao.
Collected the data: Chao Xu, Zekun Li.
Contributed data or analysis tools: Chao Xu, Zekun Li, Yueying Shan, Yanfang Yang.
Performed the analysis: Chunhua She, Tianxing Zhao, Yongjie Xie, Guangcong Shen, Boyang Fu, Bo Ni, Jinlong Pei, Chenyang Meng, Tiansuo Zhao, Guannan Sheng, Song Gao, Liangliang Wu, Hongwei Wang, Kaiyuan Wang, Chengqi Deng, Antao Chang, Lei Shi, Chongbiao Huang, Shengyu Yang, Jun Yu.
Wrote the paper: Chao Xu, Zekun Li, Xiuchao Wang.

Data availability statement

The data generated in this study are available upon request from the corresponding author.

References

1. Siegel RL, Miller KD, Fuchs HE, Jemal A. Cancer statistics, 2022. CA Cancer J Clin. 2022; 72: 7-33.
2. Wood LD, Canto MI, Jaffee EM, Simeone DM. Pancreatic cancer: pathogenesis, screening, diagnosis, and treatment. Gastroenterology. 2022; 163: 386-402.e1.
3. Tempero MA, Malafa MP, Al-Hawary M, Behrman SW, Benson AB, Cardin DB, et al. Pancreatic adenocarcinoma, version 2.2021, NCCN Clinical Practice Guidelines in Oncology. J Natl Compr Canc Netw. 2021; 19: 439-57.
4. Shukla SK, Purohit V, Mehla K, Gunda V, Chaika NV, Vernucci E, et al. MUC1 and HIF-1alpha signaling crosstalk induces anabolic glucose metabolism to impart gemcitabine resistance to pancreatic cancer. Cancer Cell. 2017; 32: 71-87.e7.
5. Wilkes JG, O'Leary BR, Du J, Klinger AR, Sibenaller ZA, Doskey CM, et al. Pharmacologic ascorbate (P-AscH$^-$) suppresses hypoxia-inducible factor-1α (HIF-1α) in pancreatic adenocarcinoma. Clin Exp Metastasis. 2018; 35: 37-51.
6. Choudhry H, Harris AL. Advances in hypoxia-inducible factor biology. Cell Metab. 2018; 27: 281-98.
7. Zhao X, Gao S, Ren H, Sun W, Zhang H, Sun J, et al. Hypoxia-inducible factor-1 promotes pancreatic ductal adenocarcinoma invasion and metastasis by activating transcription of the actin-bundling protein fascin. Cancer Res. 2014; 74: 2455-64.
8. Zhao T, Ren H, Li J, Chen J, Zhang H, Xin W, et al. LASP1 is a HIF1α target gene critical for metastasis of pancreatic cancer. Cancer Res. 2015; 75: 111-9.
9. Huang C, Li Y, Li Z, Xu Y, Li N, Ge Y, et al. LIMS1 promotes pancreatic cancer cell survival under oxygen-glucose deprivation conditions by enhancing HIF1A protein translation. Clin Cancer Res. 2019; 25: 4091-103.
10. Lang J, Zhao X, Wang X, Zhao Y, Li Y, Zhao R, et al. Targeted co-delivery of the iron chelator deferoxamine and a HIF1α inhibitor impairs pancreatic tumor growth. ACS Nano. 2019; 13: 2176-89.
11. Zhao X, Li F, Li Y, Wang H, Ren H, Chen J, et al. Co-delivery of HIF1α siRNA and gemcitabine via biocompatible lipid-polymer hybrid nanoparticles for effective treatment of pancreatic cancer. Biomaterials. 2015; 46: 13-25.
12. Sun H, Zhang D, Huang C, Guo Y, Yang Z, Yao N, et al. Hypoxic microenvironment induced spatial transcriptome changes in pancreatic cancer. Cancer Biol Med. 2021; 18: 616-30.
13. Zhang X, He C, Xiang G. Engineering nanomedicines to inhibit hypoxia-inducible factor-1 for cancer therapy. Cancer Lett. 2022; 530: 110-27.
14. McDonald PC, Chafe SC, Brown WS, Saberi S, Swayampakula M, Venkateswaran G, et al. Regulation of pH by carbonic anhydrase 9 mediates survival of pancreatic cancer cells with activated KRAS in response to hypoxia. Gastroenterology. 2019; 157: 823-37.
15. Flinn IW, Hillmen P, Montillo M, Nagy Z, Illés Á, Etienne G, et al. The phase 3 DUO trial: duvelisib vs ofatumumab in relapsed and refractory CLL/SLL. Blood. 2018; 132: 2446-55.

16. André F, Ciruelos E, Rubovszky G, Campone M, Loibl S, Rugo HS, et al. Alpelisib for *PIK3CA*-mutated, hormone receptor-positive advanced breast cancer. N Engl J Med. 2019; 380: 1929-40.
17. O'Neil BH, Scott AJ, Ma WW, Cohen SJ, Aisner DL, Menter AR, et al. A phase II/III randomized study to compare the efficacy and safety of rigosertib plus gemcitabine versus gemcitabine alone in patients with previously untreated metastatic pancreatic cancer. Ann Oncol. 2015; 26: 1923-9.
18. Jo DH, An H, Chang DJ, Baek YY, Cho CS, Jun HO, et al. Hypoxia-mediated retinal neovascularization and vascular leakage in diabetic retina is suppressed by HIF-1α destabilization by SH-1242 and SH-1280, novel hsp90 inhibitors. J Mol Med (Berl). 2014; 92: 1083-92.
19. Ichikawa D, Nakamura M, Murota W, Osawa S, Matsushita M, Yanagawa H, et al. A phenylphthalimide derivative, TC11, induces apoptosis by degrading MCL1 in multiple myeloma cells. Biochem Biophys Res Commun. 2020; 521: 252-8.
20. Wang X, Li Y, Li Z, Lin S, Wang H, Sun J, et al. Mitochondrial calcium uniporter drives metastasis and confers a targetable cystine dependency in pancreatic cancer. Cancer Res. 2022; 82: 2254-68.
21. Hou P, Chen F, Yong H, Lin T, Li J, Pan Y, et al. PTBP3 contributes to colorectal cancer growth and metastasis via translational activation of HIF-1α. J Exp Clin Cancer Res. 2019; 38: 301.
22. Luo J, Sun P, Zhang X, Lin G, Xin Q, Niu Y, et al. Canagliflozin modulates hypoxia-induced metastasis, angiogenesis and glycolysis by decreasing HIF-1α protein synthesis via AKT/mTOR pathway. Int J Mol Sci. 2021; 22: 13336.
23. Fallah J, Rini BI. HIF inhibitors: status of current clinical development. Curr Oncol Rep. 2019; 21: 6.
24. Albadari N, Deng S, Li W. The transcriptional factors HIF-1 and HIF-2 and their novel inhibitors in cancer therapy. Expert Opin Drug Discov. 2019; 14: 667-82.
25. Semenza GL. Targeting HIF-1 for cancer therapy. Nat Rev Cancer. 2003; 3: 721-32.
26. Harris B, Saleem S, Cook N, Searle E. Targeting hypoxia in solid and haematological malignancies. J Exp Clin Cancer Res. 2022; 41: 318.
27. Liu M, Zhong J, Zeng Z, Huang K, Ye Z, Deng S, et al. Hypoxia-induced feedback of HIF-1α and lncRNA-CF129 contributes to pancreatic cancer progression through stabilization of p53 protein. Theranostics. 2019; 9: 4795-810.
28. Craven KE, Gore J, Korc M. Overview of pre-clinical and clinical studies targeting angiogenesis in pancreatic ductal adenocarcinoma. Cancer Lett. 2016; 381: 201-10.
29. Xia Y, Choi H-K, Lee K. Recent advances in hypoxia-inducible factor (HIF)-1 inhibitors. Eur J Med Chem. 2012; 49: 24-40.
30. Groot AJ, Gort EH, van der Wall E, van Diest PJ, Vooijs M. Conditional inactivation of HIF-1 using intrabodies. Cell Oncol. 2008; 30: 397-409.
31. Liu X-Q, Xiong M-H, Shu X-T, Tang R-Z, Wang J. Therapeutic delivery of siRNA silencing HIF-1 alpha with micellar nanoparticles inhibits hypoxic tumor growth. Mol Pharm. 2012; 9: 2863-74.
32. Klein M, Eslami-Mossallam B, Arroyo DG, Depken M. Hybridization kinetics explains CRISPR-Cas off-targeting rules. Cell Rep. 2018; 22: 1413-23.
33. Hyun S, Shin D. Small-molecule inhibitors and Degraders Targeting KRAS-Driven cancers. Int J Mol Sci. 2021; 22: 12142.
34. Zhang Z, Yao L, Yang J, Wang Z, Du G. PI3K/Akt and HIF-1 signaling pathway in hypoxia-ischemia (Review). Mol Med Rep. 2018; 18: 3547-54.
35. Mabuchi S, Altomare DA, Cheung M, Zhang L, Poulikakos PI, Hensley HH, et al. RAD001 inhibits human ovarian cancer cell proliferation, enhances cisplatin-induced apoptosis, and prolongs survival in an ovarian cancer model. Clin Cancer Res. 2007; 13: 4261-70.
36. Jung KH, Choi MJ, Hong S, Lee H, Hong SW, Zheng HM, et al. HS-116, a novel phosphatidylinositol 3-kinase inhibitor induces apoptosis and suppresses angiogenesis of hepatocellular carcinoma through inhibition of the PI3K/AKT/mTOR pathway. Cancer Lett. 2012; 316: 187-95.
37. Li GY, Jung KH, Lee H, Son MK, Seo J, Hong SW, et al. A novel imidazopyridine derivative, HS-106, induces apoptosis of breast cancer cells and represses angiogenesis by targeting the PI3K/mTOR pathway. Cancer Lett. 2013; 329: 59-67.
38. Lee JH, Lee H, Yun SM, Jung KH, Jeong Y, Yan HH, et al. IPD-196, a novel phosphatidylinositol 3-kinase inhibitor with potent anticancer activity against hepatocellular carcinoma. Cancer Lett. 2013; 329: 99-108.
39. Sun HL, Liu YN, Huang YT, Pan SL, Huang DY, Guh JH, et al. YC-1 inhibits HIF-1 expression in prostate cancer cells: contribution of Akt/NF-kappaB signaling to HIF-1alpha accumulation during hypoxia. Oncogene. 2007; 26: 3941-51.
40. Jiang BH, Jiang G, Zheng JZ, Lu Z, Hunter T, Vogt PK. Phosphatidylinositol 3-kinase signaling controls levels of hypoxia-inducible factor 1. Cell Growth Differ. 2001; 12: 363-9.
41. Chen D, Wassel RA, Hu Y, Stanley A, Chen Y, Farjo R, et al. Therapeutic effects of a novel HIF-1 inhibitor CLT003 on diabetic macular edema. Invest Ophthalmol Vis Sci. 2009; 50: 61.
42. Wu Q, You L, Nepovimova E, Heger Z, Wu W, Kuca K, et al. Hypoxia-inducible factors: master regulators of hypoxic tumor immune escape. J Hematol Oncol. 2022; 15: 77.

Cite this article as: Xu C, Li Z, Shan Y, She C, Yang Y, Zhou T, et al. CLT-003 exerts anti-tumor activity in pancreatic cancer by blocking the PI3K/AKT/HIF-1α pathway. Cancer Biol Med. 2025; 22: 1558-1577. doi: 10.20892/j.issn.2095-3941.2025.0058